Polyhedron 28 (2009) 3891–3898

Contents lists available at ScienceDirect

Polyhedron

journal homepage: www.elsevier.com/locate/poly

# Synthesis, spectroscopic and structural characterizations of two new complexes of ruthenium with 2-(hydroxymethyl)benzimidazole and 1,10-phenanthroline ligands

J.G. Małecki [a,*], R. Kruszynski [b], Z. Mazurak [c]

[a] *Department of Inorganic and Coordination Chemistry, Institute of Chemistry, University of Silesia, 9th Szkolna St., 40-006 Katowice, Poland*
[b] *X-ray Crystallography Laboratory, Institute of General and Ecological Chemistry, Technical University of Łódź, 116 Żeromski St., 90-924 Łódź, Poland*
[c] *Polish Academy of Sciences, Centre of Polymer Chemistry, M. Sklodowskiej-Curie 34, Zabrze 41-819, Poland*

ARTICLE INFO

*Article history:*
Received 6 July 2009
Accepted 31 August 2009
Available online 27 September 2009

*Keywords:*
Ruthenium hydride carbonyl complexes
2-(Hydroxymethyl)benzimidazole
1,10-Phenanthroline
X-ray structure
UV–Vis
Luminescence
DFT
TDFFT

ABSTRACT

The complexes $[RuCl(CO)(PPh_3)_2(HBIm)]$ and $[RuH(CO)(PPh_3)_2(1{,}10\text{-phen})]Cl\cdot H_2O\cdot(CH_3)_2O$ have been prepared and studied by IR and UV–Vis spectroscopy, and X-ray crystallography. The complexes were prepared in the reactions of $[RuHCl(CO)(PPh_3)_3]$ with 2-(hydroxymethyl)benzimidazole or 1,10-phenanthroline two hydrate in acetone. The electronic spectra of the obtained compounds have been calculated using the TDDFT method. The luminescence properties of these complexes were examined.

## 1. Introduction

The study of spectroscopic (particularly UV–Vis) and luminescence properties of Ru(II) complexes is an ongoing and active area of research, mainly concerning applications of these compounds in energy conversion and as sensors. In most of these complexes, the ligands are N-heterocyclic imines involving imidazole and phenanthroline. The wide interest is this field originates from a very rich redox chemistry and photophysics of these compounds. Even a small change in the coordination environment around ruthenium plays a key role in altering the redox properties of the complexes. Thus complexation of ruthenium by various ligands is very interesting and widely studied [1–7].

The coordination compounds of transition and non-transition metals containing 8-hydroxyquinoline complexes are also very interesting due to their applications in OLED materials [8–9]. 8-Hydroxyquinoline is also commonly used for analytical determination of metals such as $Al^{3+}$, $Ga^{3+}$, $Pd^{2+}$ [10]. Due to its optoelectronic efficiency, the interest in the synthesis and properties of compounds containing 8-hydroxyquinoline and transition metals lately is increasing [11–14]. Ligands containing an imidazole ring are relatively less studied but their moderate π-donor properties are interesting. Its combination with other donor atoms should in principle afford complexes with tuneable spectroscopic properties.

The studied compounds merge the benefits of ruthenium coordination compounds and complexes containing 2-(hydroxymethyl)benzimidazole or 8-hydroxyquinoline and a carbonyl group, thus their synthesis and determination of their properties was undertaken. In this paper we present the synthesis, crystal, molecular and electronic structures, including the luminescence, and spectroscopy characterization, of some new carbonyl ruthenium(II) complexes.

## 2. Experimental

All reagents were commercially available and were used without further purification.

### 2.1. Synthesis of $[RuCl(CO)(PPh_3)_2(HBIm)]$ (**1**) and $[RuH(CO)(PPh_3)_2(1{,}10\text{-phen})]Cl\cdot H_2O\cdot(CH_3)_2O$ (**2**) (HBIm = 2-(hydroxymethyl) benzimidazole)

Both complexes were synthesized in the reaction between $[RuHCl(CO)(PPh_3)_3]$ (0.95 g; $1\times10^{-3}$ mol) and (0.15 g; $1\times10^{-3}$ mol) 2-(hydroxymethyl)benzimidazole or (0.16 g; $1\times10^{-3}$ mol) 1,10-

---

* Corresponding author.
*E-mail addresses:* gmalecki@us.edu.pl (J.G. Małecki), rafal.kruszynski@p.lodz.pl (R. Kruszynski), mazurak@cchp-pan.zabrze.pl (Z. Mazurak).

0277-5387/$ - see front matter © 2009 Elsevier Ltd. All rights reserved.
doi:10.1016/j.poly.2009.08.035

phenanthroline two hydrate in refluxing acetone (100 $cm^{-3}$). Crystals suitable for X-ray crystal analysis were obtained by slow evaporation of the reaction mixture.

### 2.2. *[RuCl(CO)(PPh$_3$)$_2$(HBIm)] (**1**)*

Yield: 71%. Colour: yellow. IR (KBr, $cm^{-1}$): 3056 $\nu_{CH}$; 2961 $\nu_{CH\text{–}phenyl}$; 1927 $\nu_{C\equiv O}$; 1622 $\nu_{CN}$; 1482 $\delta_{(C\text{–}CH \text{ in the plane})}$; 1436 $\nu_{Ph(P\text{–}Ph)}$; 1272 $\nu_{C\text{–}O}$; 1062 $\delta_{(C\text{–}CH \text{ in the plane})}$; 742 $\delta_{(C\text{–}C \text{ out of the plane})}$; 695 $\delta_{(C\text{–}C \text{ in the plane})}$. $^{31}P$ NMR ($\delta$ ppm, $CDCl_3$): 42.087 (s, $PPh_3$). UV–Vis (acetonitrile, nm): 355.4 (2.72), 281.2 (5.22), 274.3 (5.26), 243.0 sh (5.31), 211.0 (5.83). Emission: excitation 355; luminescence 450. *Anal.* Calc. for $C_{45}H_{37}ClN_2O_2P_2Ru$: C, 64.90; H, 4.74; Cl, 4.16; N, 3.29; O, 3.76; P, 7.28; Ru, 11.87. Found: C, 64.81; H, 4.66; N, 3.31%.

### 2.3. *[RuH(CO)(PPh$_3$)$_2$(1,10-phen)]Cl·H$_2$O·(CH$_3$)$_2$O (**2**)*

Yield: 65%. Colour: yellow. IR (KBr, $cm^{-1}$): 3442 $\nu_{OH}$; 3048 $\nu_{CH}$; 2903 $\nu_{CH\text{–}phenyl}$; 20 015–1923 $\nu_{C\equiv O} + \nu_{Ru\text{–}H}$; 1626 $\nu_{CN}$; 1481 $\delta_{(C\text{–}CH \text{ in the plane})}$; 1433 $\nu_{Ph(P\text{–}Ph)}$; 1225 $\nu_{C\text{–}O}$; 1095 $\delta_{(C\text{–}CH \text{ in the plane})}$; 696 $\delta_{(C\text{–}C \text{ in the plane})}$. $^{31}P$ NMR ($\delta$ ppm, $CDCl_3$): 46.153 (s, $PPh_3$). UV–Vis (acetonitrile, nm): 395.9 (2.91), 330 (sh), 272.6 (3.07), 212.0 (3.62). Emission: excitation 330, 395; luminescence 465, 467. *Anal.* Calc. for $C_{52}H_{47}ClN_2O_3P_2Ru$: C, 65.99; H, 5.01; Cl, 3.75; N, 2.96; O, 5.07; P, 6.55; Ru, 10.68. Found: C, 65.93; H, 5.03; N, 2.99%.

#### 2.3.1. *Physical measurements*

Infrared spectra were recorded on a Nicolet Magna 560 spectrophotometer in the spectral range 4000–400 $cm^{-1}$ with the sample in the form of a KBr pellet. Electronic spectra were measured on a Lab Alliance UV–Vis 8500 spectrophotometer in the range of 500–180 nm in deoxygenated acetonitrile solution. Elemental analyses (C, H, N) were performed on a Perkin–Elmer CHN-2400 analyzer. The $^{31}P$ NMR spectrum was obtained at room temperature in $CDCl_3$ using an INOVA 300 spectrometer. Luminescence measurements were made on a Jobin-Yvon (SPEX) FLUOROLOG-3.12 spectrofluorometer at room temperature.

#### 2.3.2. *DFT calculations*

The calculations were carried out using the GAUSSIAN03 [15] program. The DFT/B3LYP [16,17] method was used for the geometry optimization and electronic structure determination, and electronic spectra were calculated by the TDDFT [18] method. The calculations were performed using the DZVP basis set [19] with *f* functions with exponents 1.94722036 and 0.748930908 on the ruthenium atom, and polarization functions for all other atoms: 6-31g(2d,p) – chlorine, 6-31g$^{**}$ – carbon, nitrogen and 6-31g(d,p) – hydrogen. The PCM solvent model was used in the GAUSSIAN calculations with acetonitrile as the solvent. GaussSum 2.1 [20] was used to calculate the group contributions to the molecular orbitals and to prepare the partial density of states (PDOS) spectra. The contribution of a group to a molecular orbital was calculated using Mulliken population analysis. The PDOS spectra were created by convoluting the molecular orbital information with Gaussian curves of unit height and FWHM of 0.3 eV.

### 2.4. *Crystal structure determination and refinement*

A yellow plate crystal of [RuCl(CO)($PPh_3$)$_2$(HBIm)] (**1**) and a yellow prism of [RuH(CO)($PPh_3$)$_2$(1,10-phen)]Cl·$H_2O$·$(CH_3)_2O$ (**2**) were mounted in turn on a KM-4-CCD automatic diffractometer equipped with a CCD detector, and used for data collection. X-ray intensity data were collected with graphite monochromated Mo K$\alpha$ radiation ($\lambda$ = 0.71073 Å) at temperature of 293.0(2) K, with the $\omega$ scan mode. Exposure times of 33 s were used and Ewald sphere reflections were collected up to $2\theta = 50.06$. The unit cell parameters were determined from least-squares refinement of the setting angles of 2771 (**1**) and 7998 (**2**) strongest reflections. Details concerning crystal data and refinement are gathered in Table 1. During the data reduction, the decay correction coefficient was taken into account. Lorentz, polarization and numerical absorption corrections were applied. The structures were solved by the Patterson method. All the non-hydrogen atoms were refined anisotropically using the full-matrix, least-squares technique on $F^2$. All the hydrogen atoms were found from difference Fourier synthesis after four cycles of anisotropic refinement, and were refined as "riding" on the adjacent atom with an individual isotropic temperature factor equal to 1.2 times the value of the equivalent temperature factor of the parent atom, with geometry idealisation after each cycle. SHELXS97 [21], SHELXL97 [22] and SHELXTL [23] programs were used for all the calculations. Atomic scattering factors were those incorporated in the computer programs.

## 3. Results and discussion

The reactions of the ruthenium(II) carbonyl hydride complex [RuHCl(CO)($PPh_3$)$_3$] with 2-(hydroxymethyl)benzimidazole and 1,10-phenanthroline have been performed. Refluxing the [RuHCl(CO)($PPh_3$)$_3$] complex with a small excess of the ligands in acetone leads to the carbonyl complex [RuCl(CO)($PPh_3$)$_2$(HBIm)] and the cationic complex [RuH(CO)($PPh_3$)$_2$(1,10-phen)]Cl with good yields. Elemental analysis of the complexes is in a good agreement with their formulas. Infrared spectra of the complexes exhibit characteristic bands due to ligand rings vibrations. The $\nu_{C=N}$ band in the complexes appears around 1622 (**1**) and 1626 $cm^{-1}$ (**2**). The $\nu_{C\equiv O}$ bands in these compounds appear around 1927 (**1**) and 1923 ($\nu_{C\equiv O} + \nu_{Ru\text{–}H}$) $cm^{-1}$ (**2**). The singlet at 42.087 and 46.153 ppm for complexes (**1**) and (**2**), respectively, in the $^{31}P$ NMR spectra indi-

**Table 1**
Crystal data and structure refinement details of [RuCl(CO)($PPh_3$)$_2$(2-(HBIm)] (**1**) and [RuH(CO)($PPh_3$)$_2$(1,10-phen)]Cl (**2**).

| | **1** | **2** |
|---|---|---|
| Empirical formula | $C_{45}H_{37}ClN_2O_2P_2Ru$ | $C_{52}H_{47}ClN_2O_3P_2Ru$ |
| Formula weight | 836.23 | 946.38 |
| *T* (K) | 293.0(2) | 293.0(2) |
| Crystal system | orthorhombic | triclinic |
| Space group | *Pnma* | $P\bar{1}$ |
| *Unit cell dimensions* | | |
| *a* (Å) | 16.908(15) | 13.622(4) |
| *b* (Å) | 23.845(2) | 13.675(6) |
| *c* (Å) | 9.8420(9) | 14.985(5) |
| $\alpha$ (°) | | 102.824(3) |
| $\beta$ (°) | | 103.244(3) |
| $\gamma$ (°) | | 116.323(4) |
| *V* ($Å^3$) | 3968.0(6) | 2261.8(14) |
| *Z* | 4 | 2 |
| Calculated density ($Mg/m^3$) | 1.400 | 1.390 |
| Absorption coefficient ($mm^{-1}$) | 0.583 | 0.522 |
| *F*(0 0 0) | 1712 | 976 |
| Crystal dimensions (mm) | | $0.097 \times 0.093 \times 0.007$ |
| $0.132 \times 0.079 \times 0.070$ | | |
| $\theta$ Range for data collection (°) | 1.71–25.03 | 1.76–25.03 |
| Index ranges | $-20 \leqslant h \leqslant 20$ | $-16 \leqslant h \leqslant 16$ |
| | $-28 \leqslant k \leqslant 28$ | $-15 \leqslant k \leqslant 16$ |
| | $-11 \leqslant l \leqslant 11$ | $-16 \leqslant l \leqslant 17$ |
| Reflections collected | 73 253 | 23 194 |
| Independent reflections [$R_{(int)}$] | 2771 [0.0881] | 7998 [0.0537] |
| Data/restraints/parameters | 3603/0/262 | 7998/0/552 |
| Goodness-of-fit (GOF) on $F^2$ | 0.961 | 0.887 |
| Final *R* indices [$I > 2\sigma(I)$] | $R_1 = 0.0398$ | $R_1 = 0.0336$ |
| | $wR_2 = 0.0981$ | $wR_2 = 0.0715$ |
| *R* indices (all data) | $R_1 = 0.0599$ | $R_1 = 0.0631$ |
| | $wR_2 = 0.1039$ | $wR_2 = 0.0854$ |
| Largest difference in peak and hole (e $Å^{-3}$) | 1.753 and −0.970 | 0.589 and −0.631 |

cated both the triphenylphosphine ligands in the studied compounds are equivalent and are mutually *trans* disposed.

### 3.1. Crystal structure

The $[RuCl(CO)(PPh_3)_2(HBIm)]$ (**1**) complex crystallises in the orthorhombic space group Pnma, and the $[RuH(CO)(PPh_3)_2(1,10\text{-}phen)]Cl\cdot H_2O\cdot (CH_3)_2O$ (**2**) complex crystallises in the $P\bar{1}$ triclinic space group. The molecular structures of these compounds are shown in Figs. 1 and 2 (structural drawings are presented in Figs. 3 and 4). Selected bond lengths and angles are listed in Tables 2 and 3. In both studied complexes the ruthenium atoms have a distorted octahedral environment with *trans* triphenylphosphine ligands (angle P–Ru–P 176.51(4)° **1** and 166.36(3)° **2**). The O and N donor atoms of 2-(hydroxymethyl)benzimidazole in complex **1** are in *trans* positions to the carbonyl (C(27)–Ru(1)–O(1)

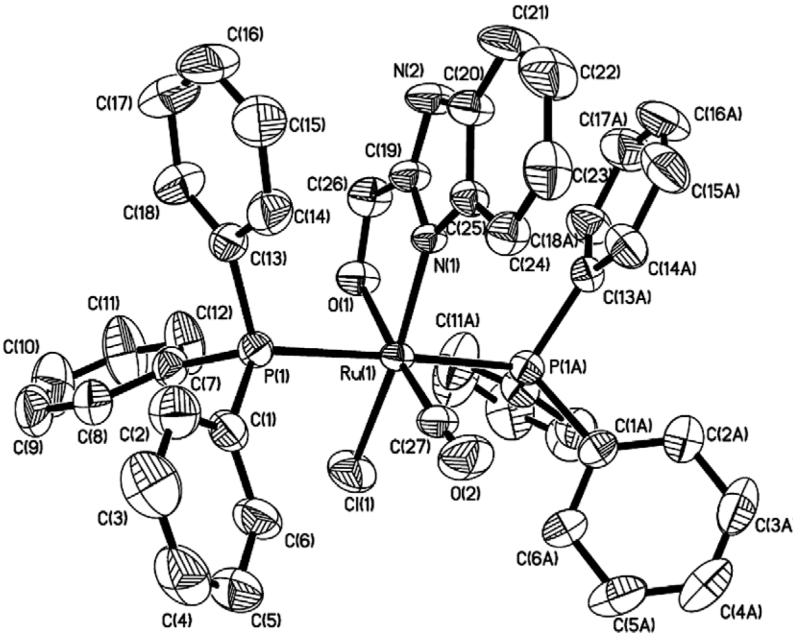

**Fig. 1.** ORTEP drawing of $[RuCl(CO)(PPh_3)_2(HBIm)]$ with 50% probability thermal ellipsoids. Hydrogen atoms are omitted for clarity.

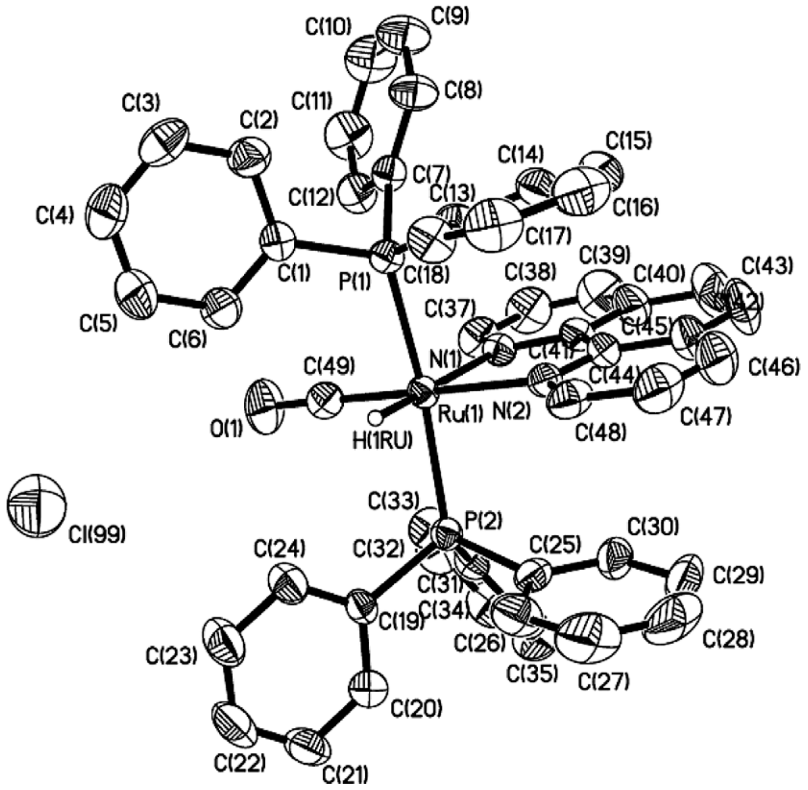

**Fig. 2.** ORTEP drawing of $[RuH(CO)(PPh_3)_2(1,10\text{-}phen)]Cl$ with 50% probability thermal ellipsoids. Hydrogen atoms (except the Ru–H) and solvents are omitted for clarity.

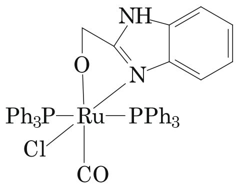

**Fig. 3.** Structural drawing of [RuCl(CO)$(PPh_3)_2$(HBIm)].

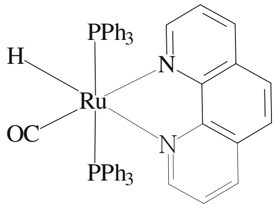

**Fig. 4.** Structural drawing of [RuH(CO)$(PPh_3)_2$(1,10-phen)]Cl.

**Table 2**
Selected bond lengths (Å) and angles (°) for [RuCl(CO)$(PPh_3)_2$(HBIm)] (**1**) with the optimized geometry values.

| | Exp. | Calc. |
|---|---|---|
| *Bond lengths (Å)* | | |
| Ru(1)–N(1) | 2.058(3) | 2.133 |
| Ru(1)–O(1) | 2.107(3) | 2.154 |
| Ru(1)–P(1) | 2.399(8) | 2.472 |
| Ru(1)–P(2) | 2.399(8) | 2.472 |
| Ru(1)–Cl(1) | 2.407(13) | 2.461 |
| Ru(1)–C(27) | 1.845(6) | 1.862 |
| C(27)–O(1) | 1.111(6) | 1.163 |
| Ru(1)–O(1) | 2.107(3) | 2.154 |
| *Angles (°)* | | |
| C(27)–Ru(1)–N(1) | 95.82(18) | 97.48 |
| C(27)–Ru(1)–O(1) | 174.38(17) | 174.91 |
| N(1)–Ru(1)–O(1) | 78.56(13) | 77.43 |
| C(27)–Ru(1)–P(1) | 90.70(2) | 92.90 |
| N(1)–Ru(1)–P(1) | 91.52(2) | 92.96 |
| O(1)–Ru(1)–P(1) | 89.46(2) | 87.41 |
| C(27)–Ru(1)–Cl(1) | 95.31(16) | 91.67 |
| N(1)–Ru(1)–Cl(1) | 168.87(10) | 170.86 |
| O(1)–Ru(1)–Cl(1) | 90.31(10) | 93.43 |
| P(1)–Ru(1)–Cl(1) | 88.34(2) | 86.55 |
| P(1)–Ru(1)–P(1A) | 176.51(4) | 171.09 |

174.38(17)°) and chloride (N(1)–Ru(1)–Cl(1) 168.87(10)°) ligands, respectively. In complex **2**, the nitrogen donors of 1,10-phenanthroline are in *trans* positions to the carbonyl and hydride ligands.

The C(27)–O(1) bond in complex **1** shows some shortening in comparison with typical distances in CO substituents, but similar distances can be found in several compounds [24–41]. The Ru(1)–N(1) bond distance is longer in complex **2** compared with Ru(1)–N(2), due to the *trans* effect of the hydride ligand. All Ru–ligand distances in both studied compounds are normal and comparable with distances in other ruthenium complexes containing the heterocyclic ligands.

The conformation of molecule **1** is stabilised by two intramolecular weak hydrogen bonds, linking coordinated O(1) and phenyl C(12) (D···A distance 3.067(5) Å and D–H···A angle 152.6°) and carbonyl oxygen O(2) and carbon C(24) from the benzimidazole ligand (D···A distance 3.419(7) Å and D–H···A angle 150.1°).

### 3.1.1. Optimized geometries

The geometries of the studied complexes were optimized in singlet states using the DFT method with the B3LYP functional. The optimized geometric parameters are gathered in Tables 2 and 3. In general, the predicted bond lengths and angles are in a good agreement with the values based on the X-ray crystal structure data, and the general trends observed in the experimental data are well reproduced in the calculations.

**Table 3**
Selected bond lengths (Å) and angles (°) for [RuH(CO)$(PPh_3)_2$(1,10-phen)]Cl (**2**) with the optimized geometry values.

| | Exp. | Calc. |
|---|---|---|
| *Bond lengths (Å)* | | |
| Ru(1)–N(1) | 2.174(3) | 2.255 |
| Ru(1)–N(2) | 2.133(3) | 2.183 |
| Ru(1)–P(1) | 2.359(9) | 2.451 |
| Ru(1)–P(2) | 2.364(9) | 2.451 |
| Ru(1)–C(49) | 1.828(4) | 1.870 |
| C(49)–O(1) | 1.153(4) | 1.161 |
| Ru(1)–H(1Ru) | 1.513 | 1.611 |
| *Angles (°)* | | |
| C(49)–Ru(1)–N(1) | 101.45(13) | 103.97 |
| C(49)–Ru(1)–N(2) | 178.05(13) | 179.33 |
| N(1)–Ru(1)–N(2) | 76.60(11) | 75.36 |
| C(49)–Ru(1)–P(1) | 90.78(11) | 88.39 |
| C(49)–Ru(1)–P(2) | 90.26(11) | 88.38 |
| N(1)–Ru(1)–P(1) | 96.22(8) | 95.07 |
| N(1)–Ru(1)–P(2) | 96.90(8) | 95.07 |
| N(2)–Ru(1)–P(1) | 89.30(8) | 91.67 |
| N(2)–Ru(1)–P(2) | 90.11(7) | 91.68 |
| P(1)–Ru(1)–P(2) | 166.36(3) | 169.83 |
| C(49)–Ru(1)–H(1RU) | 85.7 | 88.70 |
| N(2)–Ru(1)–H(1RU) | 96.3 | 91.98 |
| N(1)–Ru(1)–H(1RU) | 172.2 | 167.34 |
| P(1)–Ru(1)–H(1RU) | 80.4 | 85.15 |
| P(2)–Ru(1)–H(1RU) | 86.2 | 85.14 |

The maximum differences between the optimized and experimental geometries of the studied compounds are visible in the Ru(1)–N(1) distance (~0.075 Å) for complex **1** Ru(1)–P(1) (~0.092 Å) for **2** and in the angle P(1)–Ru(1)–P(1A), 5.4° for **1**, and N(1)–Ru(1)–H(1RU), 4.9° for **2**.

### 3.1.2. Electronic structure and NBO analysis

In the studied complexes, the occupied $d_{xy}$ and $d_{xz}$ ruthenium orbitals participate in back-donation from the central ion to the carbonyl ligand. The largest contribution of the $\pi_{Ru-CO}$ bonding interaction is visible in the H-3 and H-2 orbitals for compound **1**, and H-4 and H-3 for **2**. The $\pi^{*}_{Ru-CO}$ orbitals are also distributed among several unoccupied molecular orbitals. Their contributions are visible in the L + 11 and L + 15, and L + 12 and L + 15 orbitals for complexes **1** and **2**, respectively. The HOMO orbitals of the studied complexes are composed of the $d_{xz}$ ruthenium orbital. The LUMO orbitals are localised on the phosphine ligand in complex **1** and on the phenanthroline ligand in complex **2**. The $d_{z^2}$ orbital of the Ru atom makes the largest contribution into LUMO (**1**) and L + 2 (**2**), whereas L + 9, L + 11 in compound **1** and L + 15 in compounds **1** and **2** have $d_{x^2-y^2}$ character. The energy and character of the selected frontier molecular orbitals are gathered in Table 4. In the frontier region, neighboring orbitals are often closely spaced. In such cases, consideration of only the HOMO and LUMO may not yield a realistic description of the frontier orbitals. For this reason, partial density of states (PDOS) diagrams, which incorporate a degree of overlap between the curves convoluted from neighboring energy levels, can give a more representative picture of the nature of the frontier orbitals. The PDOS diagrams obtained are shown in Fig. 5. The HOMO−LUMO gaps are 4.06 and 3.62 eV for **1** and **2**, respectively.

Basing on the NBO theory [42], occupancy and hybridization of the calculated natural bond orbital between the ruthenium and

**Table 4**
The energies and characters of selected molecular orbitals for complexes **1** and **2**.

| | $[RuCl(CO)(PPh_3)_2(2\text{-(hydroxymetyl)benzimidazole})]$ (**1**) | | $[RuHCl(CO)(phen)(PPh_3)_2]^+$ (**2**) | |
|---|---|---|---|---|
| | *E* (eV) | Character | *E* (eV) | Character |
| HOMO−19 | −7.470 | $d_{Ru}$; $\pi_{Cl}$ | −11.057 | $\pi_{phosphine}(59)$; $\pi_{phen}(32)$ |
| HOMO−18 | −7.172 | $d_{Ru}$; $\pi_{phosphine}$ | −10.277 | $\pi_{phosphine}$ |
| HOMO−17 | −7.075 | $\pi_{phosphine}$ | −9.938 | $\pi_{phen}$ |
| HOMO−16 | −7.000 | $\pi_{phosphine}$ | −9.701 | $\pi_{phen}$ |
| HOMO−15 | −6.956 | $\pi_{phosphine}$ | −9.442 | $\pi_{phosphine}$ |
| HOMO−14 | −6.900 | $\pi_{phosphine}$ | −9.346 | $\pi_{phen}$ |
| HOMO−13 | −6.869 | $\pi_{phosphine}$ | −9.343 | $\pi_{phosphine}$ |
| HOMO−12 | −6.830 | $\pi_{phosphine}$; $\pi_{HMBI}$ | −9.231 | $\pi_{phosphine}$ |
| HOMO−11 | −6.788 | $\pi_{phosphine}$ | −9.193 | $\pi_{phosphine}$ |
| HOMO−10 | −6.777 | $\pi_{phosphine}$; $\pi_{HMBI}$ | −9.151 | $\pi_{phosphine}$ |
| HOMO−9 | −6.678 | $\pi_{phosphine}$; $\pi_{HMBI}$ | −9.105 | $\pi_{phosphine}$ |
| HOMO−8 | −6.647 | $\pi_{HMBI}$ | −9.099 | $\pi_{phosphine}$ |
| HOMO−7 | −6.634 | $\pi_{phosphine}$ | −9.038 | $\pi_{phosphine}$ |
| HOMO−6 | −6.560 | $\pi_{phosphine}$ | −8.945 | $\pi_{phosphine}$ |
| HOMO−5 | −6.407 | $\pi_{phosphine}$; $\pi_{HMBI}$; $\pi_{Cl}$ | −8.875 | $\pi_{phosphine}$; $d_{Ru}$ |
| HOMO−4 | −6.252 | $\pi_{phosphine}$; $d_{Ru}$ | −8.830 | $\pi_{phosphine}$; $d_{Ru}$; $\pi_{CO}$ |
| HOMO−3 | −6.092 | $n_P$; $d_{Ru}$; $\pi_{CO}$ | −8.793 | $\pi_{phosphine}$; $d_{Ru}$; $\pi_{CO}$ |
| HOMO−2 | −5.682 | $d_{Ru}$;$\pi_{CO}$ | −8.777 | $d_{Ru}$ |
| HOMO−1 | −5.542 | $d_{Ru}$; $\pi^*_{Cl}$ | −8.598 | $d_{Ru}$ |
| HOMO | −5.153 | $d_{Ru}$ | −8.207 | $d_{Ru}$ |
| LUMO | −1.068 | $d_{Ru}$; $\pi^*_{phosphine}$ | −4.587 | $\pi^*_{phen}$ |
| LUMO +1 | −0.629 | $\pi^*_{HMBI}$ | −4.464 | $\pi_{phen}$ |
| LUMO+2 | −0.601 | $\pi^*_{phosphine}$ | −3.288 | $\pi^*_{phen}$; $d_{Ru}$ |
| LUMO+3 | −0.546 | $\pi^*_{phosphine}$ | −3.227 | $\pi^*_{phen}$ |
| LUMO+4 | −0.522 | $\pi^*_{phosphine}$ | −2.936 | d; $\pi^*_{phosphine}$ |
| LUMO+5 | −0.364 | $\pi^*_{phosphine}$ | −2.857 | $\pi^*_{phosphine}$ |
| LUMO+6 | −0.287 | $\pi^*_{phosphine}$ | −2.841 | $\pi^*_{phosphine}$ |
| LUMO+7 | −0.282 | $\pi^*_{phosphine}$ | −2.803 | $\pi^*_{phosphine}$ |
| LUMO+8 | −0.183 | $\pi^*_{phosphine}$ | −2.547 | $\pi^*_{phosphine}$ |
| LUMO+9 | −0.121 | $d_{Ru}$; $\pi^*_{phosphine}$; $\pi^*_{CO}$ | −2.528 | $\pi^*_{phosphine}$ |
| LUMO+10 | 0.041 | $\pi^*_{phosphine}$; $\pi^*_{HMBI}$ | −2.456 | $\pi^*_{phosphine}$; $\pi^*_{phen}$ |
| LUMO+11 | 0.057 | $d_{Ru}$; $\pi^*_{phosphine}$; $\pi^*_{CO}$ | −2.440 | $\pi^*_{phosphine}$ |
| LUMO+12 | 0.183 | $\pi^*_{phosphine}$ | −2.404 | $\pi^*_{phosphine}$; $\pi^*_{CO}$ |
| LUMO+13 | 0.189 | $\pi^*_{phosphine}$ | −2.262 | $\pi^*_{phosphine}$ |
| LUMO+14 | 0.189 | $\pi^*_{phosphine}$ | −2.219 | $\pi^*_{phosphine}$ |
| LUMO+15 | 0.304 | $d_{Ru}$; $\pi^*_{phosphine}$; $\pi^*_{CO}$ | −2.150 | $d_{Ru}$; $\pi^*_{phosphine}$; $\pi^*_{CO}$ |

the hydrido ligand in the complex **2** is 1.923 and $0.734(sd)_{Ru} + 0.679(s)_H$, respectively; occupancy of the antibonding orbital of Ru–H is 0.328. The occupancies and hybridizations of the Ru–CO bond are as follows: 1.970 (antibonding 0.325) and $0.548(sd^{5.64})_{Ru} + 0.836(sp^{0.54})_C$ for complex **1**; 1.979 (antibonding 0.410) and $0.576(sd^{9.75})_{Ru} + 0.817(sp^{0.54})_C$ for **2**.

The stabilization energy[1] calculated in these analyses has shown that the lone pairs localized on the ruthenium atom in complex **1** donate the charge to the ruthenium carbonyl bond, and the stabilization energy ($\Delta E_{ij}$) is 464.17 kcal/mol. The interaction between the Ru–P bond and the ruthenium $d_{z^2}$ orbital has an energy close to 135.46 kcal/mol. The stabilization energy calculated in this analysis for the complex has shown that the lone pairs localized on the chlorine ligand donate the charge to the ruthenium *d* orbital, and the stabilization energy ($\Delta E_{ij}$) is 112.25 kcal/mol. For complex **2**, the donations of charge are mainly visible between ruthenium–carbonyl and hydride ligand bonds and Ru d orbitals; the stabilization energies are close to 505.91 and 297.20 kcal/mol, respectively.

In both studied complexes, ruthenium is formally +2, but the calculated charges on the ruthenium atom are 0.284 in complex **1** and is close to zero with a negative sign (−0.067) in compound **2**. The charges on the carbon atom of the carbonyl ligand are positive (0.569 (**1**), 0.568 (**2**)), whereas the oxygen atoms are negatively charged (−0.505 (**1**), −0.482 (**2**)). The charge of hydride ligand in complex **2** is calculated to be −0.064. The occupancies of the ruthenium *d* orbitals, obtained from NBO analysis, are as follows: $d_{xy}$ – 1.92; $d_{xz}$ – 1.77; $d_{yz}$ – 1.72; $d_{z^2}$ – 0.96; $d_{x^2-y^2}$ – 0.99 and $d_{xy}$ – 1.79; $d_{xz}$ – 1.85; $d_{yz}$ – 1.10; $d_{z^2}$ – 1.67; $d_{x^2-y^2}$ – 1.26 for **1** and **2**, respectively.

### 3.1.3. Electronic spectra

The experimental and calculated (using TD–DFT theory) electronic spectra of $[RuCl(CO)(PPh_3)_2(HOBIm)]$ (**1**) and $[RuH(CO)(PPh_3)_2(1,10\text{-phen})]Cl$ (**2**) are presented in Figs. 6 and 7. The assignments of the calculated transitions to the experimental bands are based on the criterion of energy and oscillator strength of the calculated transitions. In the description of the electronic transitions, only the main components of the molecular orbital are taken into consideration.

In both the studied complexes, 120 electronic transitions were calculated using the TDDFT method and they do not comprise all the experimental absorption bands. The UV–Vis spectra were calculated up to ∼220 nm, so considering that the solution spectra of the $PPh_3$ and N-heterocyclic ligands exhibit intense absorption bands in the 260–200 nm region, some intraligand and interligand transitions are expected to be found at higher energies in the calculations.

The longest wavelength experimental bands, with a maximum at 355.4 and 395.9 nm for complexes **1** and **2**, respectively, are assigned to the transitions from HOMO, HOMO−1 and HOMO−2 to LUMO and LUMO+1 orbitals. As the LUMO orbitals are composed of the $\pi^*$ orbitals of phosphine (**1**) and phenanthroline (**2**), the tran-

---

[1] $\Delta E_{ij}$ (kcal/mol) associated with delocalization is estimated by the second-order perturbative as: $\Delta E_{ij} = q_i\,(F(i,j)^2)/(\varepsilon_j - \varepsilon_i)$ where $q_i$ is the donor orbital occupancy, $\varepsilon_i$, $\varepsilon_j$ are diagonal elements (orbital energies) and $F(i,j)$ is the off-diagonal NBO Fock or Kohn–Sham matrix element.

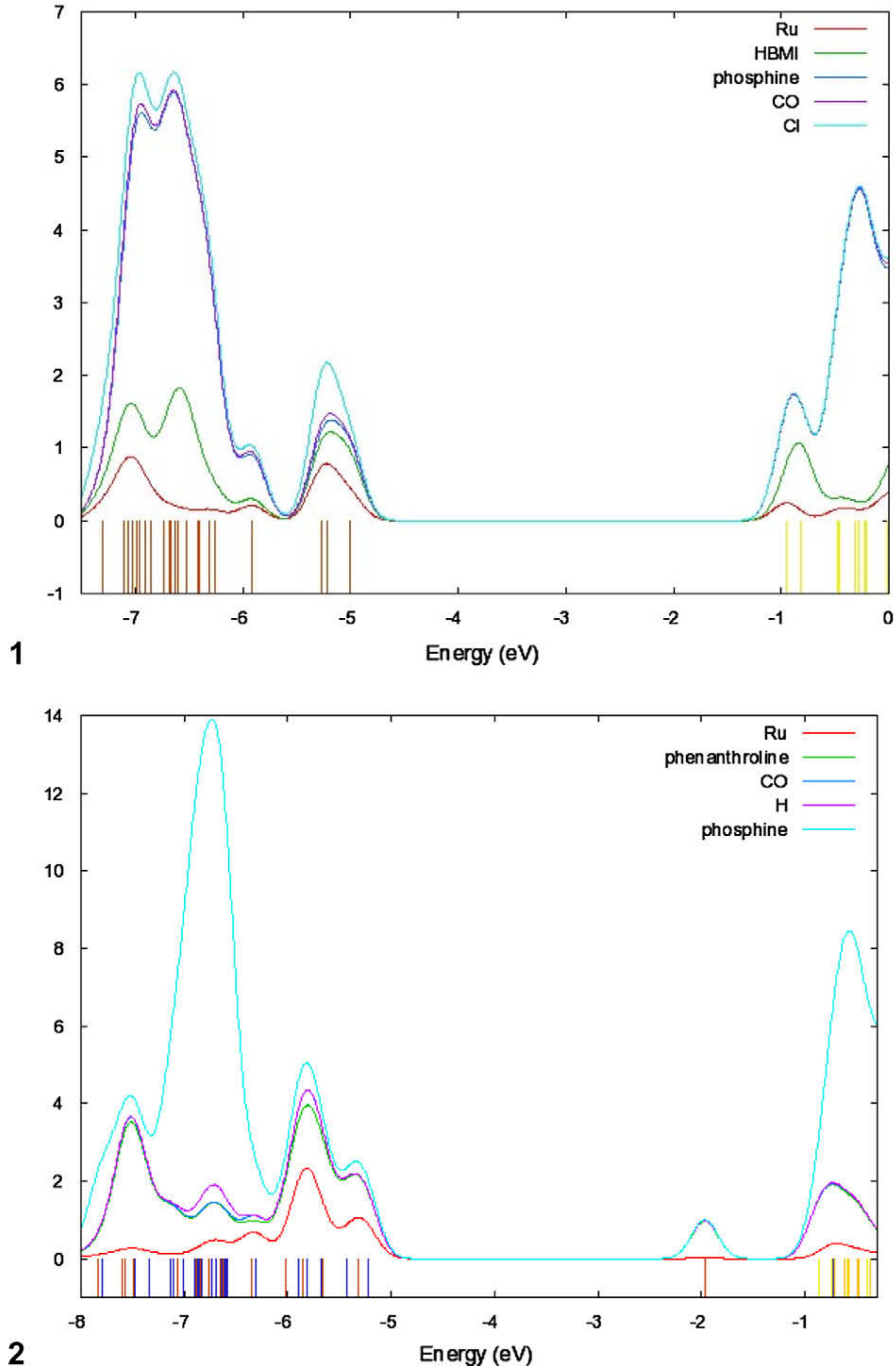

**Fig. 5.** PDOS diagrams for [RuCl(CO)(PPh$_3$)$_2$(HBIm)] (**1**) and [RuH(CO)(PPh$_3$)$_2$(1,10-phen)]Cl (**2**).

sition is of *Metal–Ligand Charge Transfer* type with a d → d (Ligand Field) contribution.

The next band, with maxima at 281.2 (5.22) and 274.3 nm for **1** and 330 (sh), 272.6 for **2** nm, is ascribed to metal–ligand charge transfer transitions ($d \rightarrow \pi^*_{PPh_3/HMBI}$; $d \rightarrow \pi^*_{phen}$). In this region, the transitions between HOMO, HOMO−1, HOMO−3 and HOMO−4 to LUMO and LUMO+2/5/6 and LUMO+11 MOs were calculated.

The calculated transition attributed to experimental one at 243.6 nm for compound **1** proceeds mainly from *d* ruthenium orbitals to $\pi^*_{Ph}$ and $\pi^*_{CO}$ orbitals with an admixture of *Ligand–Ligand Charge Transfer* transitions ($\pi_{PPh_3} \rightarrow \pi^*_{CO}$).

The intraligand transitions $\pi_{PPh_3} \rightarrow \pi^*_{PPh_3}$ were calculated to be at about 220 nm and one may assume that the experimental bands at 211.0 and 212.0 nm for complexes **1** and **2** are composed of the transitions in PPh$_3$ ligands and from $\pi \rightarrow \pi^*$ excitations in 2-(hydroxymethyl)benzimidazole and phenanthroline ligands. As it was pointed out in the literature, the TDDFT method gives such transitions at too small an energy [43–51] and we may expect also that this is the case in our calculations.

The emission properties of the studied complexes have been examined in acetonitrile solutions at room temperature. The luminescence spectra are presented in Fig. 8. For excitation at 355 nm, the emission peak was observed at 450 nm for complex **1**. Excitation of complex **2** at 395 nm gave an emission with a maximum at 465 nm. Additionally, excitation of compound **2** at 330 nm (the absorption band has MLCT character) gave an emission at

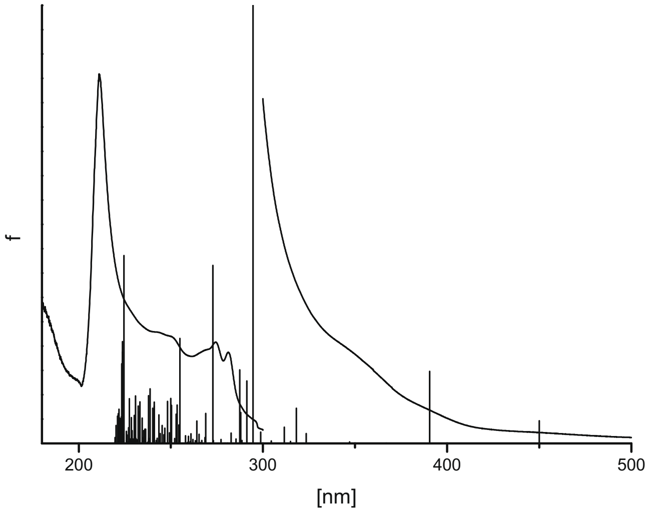

**Fig. 6.** UV–Vis spectra of [RuCl(CO)($PPh_3$)$_2$(HBIm)] with calculated singlet excited states in acetonitrile solution.

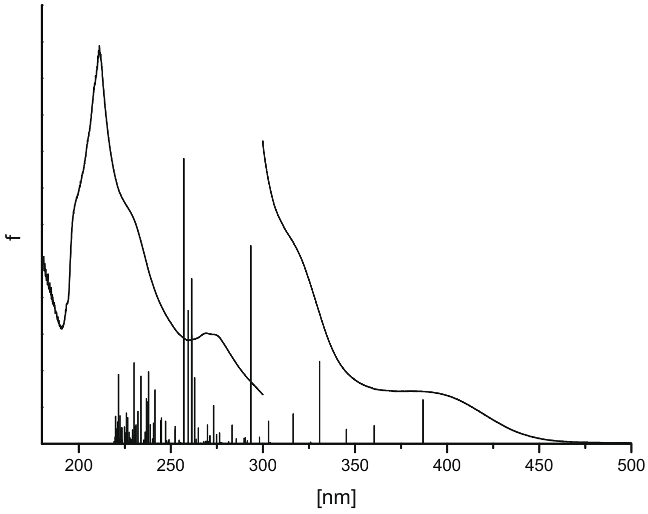

**Fig. 7.** UV–Vis spectra of [RuH(CO)($PPh_3$)$_2$(1,10-phen)]Cl with calculated singlet excited states in acetonitrile solution.

467 nm, with low intensity. In both the studied complexes, the strong emission originates from the lowest energy metal to ligand charge transfer (MLCT) state, derived from the excitation involving a $d\pi \rightarrow \pi_{\text{ligand}}$ transition (similar MLCT transitions are observed in ruthenium(II) bipyridyl complexes [52,53]). The assignment is also supported by the analysis of the frontier orbitals of the corresponding complexes, showing a partial contribution of the ligands' nature. The strong emission property makes it a potentially favorable material for emitting diode devices.

## Supplementary data

CCDC 683037 and 683130 contains the supplementary crystallographic data for [RuCl(CO)($PPh_3$)$_2$(HOBIm)] and RuH(CO)($PPh_3$)$_2$(1,10-phen)]Cl·$H_2O$·$(CH_3)_2O$. These data can be obtained free of charge via http://www.ccdc.cam.ac.uk/conts/retrieving.html, or from the Cambridge Crystallographic Data Centre, 12 Union Road, Cambridge CB2 1EZ, UK; fax: (+44) 1223-336-033; or e-mail: deposit@ccdc.cam.ac.uk.

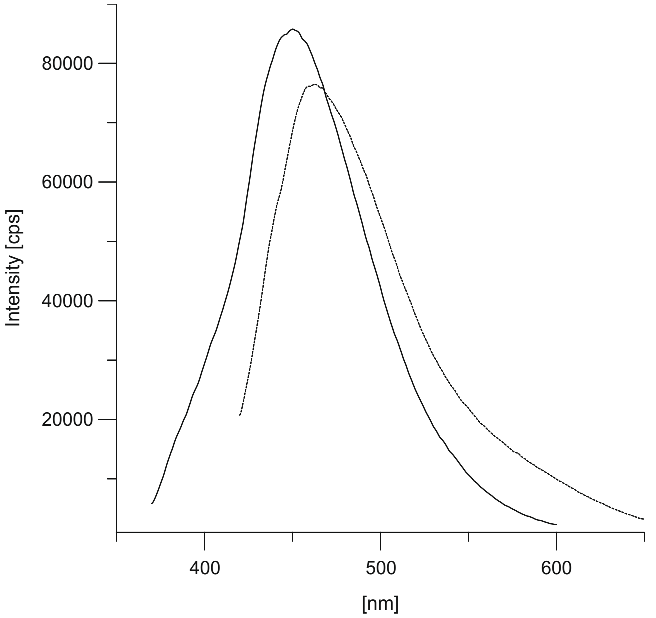

**Fig. 8.** Emission spectra of [RuCl(CO)($PPh_3$)$_2$(HBIm)] (solid line) and [RuH(CO)($PPh_3$)$_2$(1,10-phen)]Cl (dashed line).

## Acknowledgements

The crystallographic part was financed by funds allocated by the Ministry of Scientific Research and Information Technology to the Institute of General and Ecological Chemistry, Technical University of Łódź. The GAUSSIAN03 calculations were carried out in Wrocław Centre for Networking and Supercomputing, WCSS, Wrocław, Poland under calculational Grant No. 51/96.

## References

[1] J. Reedijk, in: G. Wilkinson, R.D. Gillard, J.A. MeCleverty (Eds.), Comprehensive Coordination Chemistry, vol. 2, Pergamon Press, Oxford, 1987, p. 73.
[2] K. Kalyansundaram, M. Gratzel, Coord. Chem. Rev. 177 (1998) 347.
[3] M.D. Ward, Chem. Soc. Rev. 24 (1995) 121.
[4] W.T. Wong, Coord. Chem. Rev. 131 (1994) 45.
[5] V. Balzani, A. Credi, F. Scandola, in: L. Fabbrizzi, A. Poggi (Eds.), Transition Metals in Supramolecular Chemistry, Kulwer, Dordrecht, The Netherlands, 1994, p. 1.
[6] P.A. Anderson, R.F. Anderson, M. Furue, P.C. Junk, R.F. Keene, B.T. Patterson, B.D. Yeomens, Inorg. Chem. 39 (2000) 2721.
[7] A.H. Velders, A.G. Quiroga, J.G. Haasnoot, J. Reedijk, Eur. J. Inorg. Chem. (2003) 713. and references therein.
[8] J.-F. Moulin, M. Brinkmann, A. Thierry, J.-C. Wittmann, Adv. Mater. 14 (2002) 436.
[9] L.S. Sapochak, F.E. Benincasa, R.S. Schofield, J.L. Baker, K.K.C. Riccio, D. Fogarty, H. Kohlmnn, K.F. Ferris, P. Burrows, J. Am. Chem. Soc. 124 (2002) 6119.
[10] G. Svehila, Vogels Qualitative Inorganic Analysis, Longmans, London, 1998.
[11] G.K. Lahiri, S. Bhattacharya, B.K. Ghosh, A. Chakravorty, Inorg. Chem. 26 (1987) 4324.
[12] S. Bhattacharya, Polyhedron 12 (1993) 235.
[13] M. Menon, A. Pramanik, N. Bag, A. Chakravorty, J. Chem. Soc., Dalton Trans. (1995) 1417.
[14] N.C. Pramanik, S. Bhattacharya, J. Chem. Res. (1997) 98.
[15] GAUSSIAN 03, Revision B.03, M.J. Frisch, G.W. Trucks, H.B. Schlegel, G.E. Scuseria, M.A. Robb, J.R. Cheeseman, J.A. Montgomery Jr., T. Vreven, K.N. Kudin, J.C. Burant, J.M. Millam, S.S. Iyengar, J. Tomasi, V. Barone, B. Mennucci, M. Cossi, G. Scalmani, N. Rega, G.A. Petersson, H. Nakatsuji, M. Hada, M. Ehara, K. Toyota, R. Fukuda, J. Hasegawa, M. Ishida, T. Nakajima, Y. Honda, O. Kitao, H. Nakai, M. Klene, X. Li, J. E. Knox, H.P. Hratchian, J.B. Cross, C. Adamo, J. Jaramillo, R. Gomperts, R.E. Stratmann, O. Yazyev, A.J. Austin, R. Cammi, C. Pomelli, J.W. Ochterski, P.Y. Ayala, K. Morokuma, G.A. Voth, P. Salvador, J.J. Dannenberg, V.G. Zakrzewski, S. Dapprich, A.D. Daniels, M.C. Strain, O. Farkas, D.K. Malick, A.D. Rabuck, K. Raghavachari, J.B. Foresman, J.V. Ortiz, Q. Cui, A.G. Baboul, S. Clifford, J. Cioslowski, B.B. Stefanov, G. Liu, A. Liashenko, P. Piskorz, I. Komaromi, R.L. Martin, D.J. Fox, T. Keith, M.A. Al-Laham, C.Y. Peng, A. Nanayakkara, M. Challacombe, P.M.W. Gill, B. Johnson, W. Chen, M.W. Wong, C. Gonzalez, J.A. Pople, GAUSSIAN, Inc., Pittsburgh PA, 2003.

[16] A.D. Becke, J. Chem. Phys. 98 (1993) 5648.
[17] C. Lee, W. Yang, R.G. Parr, Phys. Rev. B 37 (1988) 785.
[18] M.E. Casida, in: J.M. Seminario (Ed.), Recent Developments and Applications of Modern Density Functional Theory, Theoretical and Computational Chemistry, vol. 4, Elsevier, Amsterdam, 1996, p. 391.
[19] K. Eichkorn, F. Weigend, O. Treutler, R. Ahlrichs, Theor. Chim. Acc. 97 (1997) 119.
[20] N.M. O'Boyle, A.L. Tenderholt, K.M. Langner, J. Comp. Chem. 29 (2008) 839.
[21] G.M. Sheldrick, Acta Crystallogr. A 46 (1990) 467.
[22] G.M. Sheldrick, SHELXL97. Program for the Solution and Refinement of Crystal Structures, University of Gttingen, Germany, 1997.
[23] G.M. Sheldrick, SHELXTL: Release 4.1 for Siemens Crystallographic Research Systems (1990).
[24] C.J. Adams, M.I. Bruce, P.A. Humphrey, B.W. Skelton, A.H. White, Aust. J. Chem. 54 (2001) 325.
[25] M.F. McGuiggan, L.H. Pignolet, Cryst. Struct. Commun. 7 (1978) 583.
[26] W. Baratta, P. Da Ros, A. Del Zotto, A. Sechi, E. Zangrando, P. Rigo, Angew. Chem., Int. Ed. 43 (2004) 3584.
[27] D. Duraczynska, J.H. Nelson, J. Chem. Soc., Dalton. Trans. (2005) 92.
[28] S. Merlino, G. Montagnoli, Atti. Soc. Tosc. Sci. Nat. Pisa. 76 (1969) 335.
[29] S. Gopinathan, I.R. Unni, C. Gopinathan, V.G. Puranik, S.S. Tavale, T.N.G. Row, Polyhedron 6 (1987) 1859.
[30] S.S.D. Brown, I.D. Salter, L. Toupet, J. Chem. Soc., Dalton Trans. (1988) 757.
[31] D. Sellmann, F. Knoch, C. Wronna, Angew. Chem., Int. Ed. 27 (1988) 691.
[32] D.A. Weinberger, T.B. Higgins, C.A. Mirkin, C.L. Stern, L.M. Liable-Sands, A.L. Rheingold, J. Am. Chem. Soc. 123 (2001) 2503.
[33] T.E. Bitterwolf, M.B. Leonard, P.A. Horine, J.E. Shade, A.L. Rheingold, D.J. Staley, G.P.A. Yap, J. Organomet. Chem. 512 (1996) 11.
[34] E. Ngai-Man Ho, Wing-Tak Wong, J. Organomet. Chem. 626 (2001) 125.
[35] Y. Matsuo, E. Nakamura, Organometallics 22 (2003) 2554.
[36] S.B. Colbran, D.C. Craig, W.M. Harrison, A.E. Grimley, J. Organomet. Chem. 408 (1991) C33.
[37] H. Werner, M.A. Tena, N. Mahr, K. Peters, H.-G. von Schnering, Chem. Ber. 128 (1995) 41.
[38] M. Haukka, J. Kiviaho, M. Ahlgren, T.A. Pakkanen, Organometallics 14 (1995) 825.
[39] K. Severin, D. Koch, K. Polborn, W. Beck, Z. Anorg. Allg. Chem. 622 (1996) 562.
[40] T. Adatia, I.D. Salter, Polyhedron 15 (1996) 597.
[41] S.D. Drouin, S. Monfette, D. Amoroso, G.P.A. Yap, D.E. Fogg, Organometallics 24 (2005) 4721.
[42] J.P. Foster, F. Weinhold, J. Am. Chem. Soc. 102 (1980) 7211.
[43] A. Rosa, E.J. Baerends, S.J.A. van Gisbergen, E. van Lenthe, J.A. Groeneveld, J.G. Snijders, J. Am. Chem. Soc. 121 (1999) 10356.
[44] J.-F. Guillemoles, V. Barone, L. Joubert, C. Adamo, J. Phys. Chem. A 106 (2002) 11354.
[45] J.E. Monat, J.H. Rodriguez, J.K. McCusker, J. Phys. Chem. A 106 (2002) 7399.
[46] S. Fantacci, F. De Angelis, A. Selloni, J. Am. Chem. Soc. 125 (2003) 4381.
[47] A. Dreuw, M. Head-Gordon, J. Am. Chem. Soc. 126 (2004) 4007.
[48] A. Dreuw, J.L. Weisman, M. Head-Gordon, J. Chem. Phys. 119 (2003) 2943.
[49] O. Gritsenko, E.J. Baerends, J. Chem. Phys. 121 (2004) 655.
[50] S. Zális̆, N. Ben Amor, C. Daniel, Inorg. Chem. 43 (2004) 7978.
[51] R.S. da Silva, S.I. Gorelsky, E.S. Dodsworth, E. Tfouni, A.B.P. Lever, J. Chem. Soc., Dalton Trans. (2000) 4078.
[52] V.W.W. Yam, B.W.K. Chu, C.C. Ko, K.K. Cheung, J. Chem. Soc., Dalton Trans. (2001) 1911.
[53] B.K. Panda, K.G. Ghosh, S. Chattoppadhyay, A. Chkravoty, J. Organomet. Chem. 674 (2003) 107.